Enhanced conductance near zero voltage bias in mesoscopic superconductor-semiconductor junctions

P. H. C. Magnée, N. van der Post,* P. H. M. Kooistra, B. J. van Wees, and T. M. Klapwijk
Department of Applied Physics and Material Science Centre, University of Groningen, Nijenborgh 4, 9747 AG Groningen, The Netherlands
(Received 7 April 1994)

We have studied the conductance enhancement near zero voltage bias of double-barrier Nb-p^{++}Si-E junctions, where we chose for the counterelectrode E either Nb, Al, or W. The experiments show a large correction, $\Delta G \approx 0.1 G_N$, on the classical superconductor–insulator–normal-metal (SIN) conductance. We present measurements of the temperature, magnetic-field, and voltage dependence, and we interpret the observed results within the available theoretical models for coherent Andreev reflection, as provided by several authors.

I. INTRODUCTION

Superconductor-semiconductor devices have become a topic of intensive research in recent years. They provide excellent systems to study transport phenomena in superconductor–normal-conductor (SN) structures. Due to the superconducting energy gap Δ, nonlinear effects in the conductance are already present at very low voltages. One of the most interesting phenomena that may occur at the interface between a superconductor and a normal metal is Andreev reflection.[1] An electron, with an energy $E < \Delta$, can only penetrate the superconductor by finding a matched electron, thus leaving a hole which is (retro)reflected into the normal metal.

Blonder *et al.*[2] (BTK) describe transport across a SIN interface in terms of Andreev and normal reflection, for arbitrary transparencies Γ of the interface. In SIN, the I stands for a barrier at the interface, either due to an actual tunnel barrier, a Schottky barrier, or a Fermi-velocity mismatch between the two materials. The barrier strength is expressed with a dimensionless parameter $Z = H/\hbar v_F$, where H is the strength of the δ-function potential barrier at the interface. Octavio *et al.*[3] (OTBK) used this model to give an explanation for the subharmonic gap structures (SGS) in SNS junctions, in terms of multiple Andreev reflections, as originally proposed by Klapwijk *et al.*[4] This OTBK model, with some simplifications made by Flensberg *et al.*,[5] also explains the occurrence of a current deficit or an excess current at higher voltages, depending on the barrier strength.

For double-barrier SNS structures it is crucial to take into account phase coherent transport, especially for the description of the Josephson effect. Kastalsky *et al.*[6] reported experimental results that clearly indicate that phase coherence is also important for single SN junctions, in particular at low energies. They found an enhancement of the conductance of Nb-$In_xGa_{1-x}As$ contacts for low voltages, smaller than the superconducting energy gap Δ_{Nb}, at temperatures well below the superconducting transition temperature T_c of Nb. The enhancement was of the order of G_N, the normal state conductance, which is well beyond the small modifications usually given by quantum corrections to the conductance, e.g., due to weak localization.[7] They interpreted this effect by assuming a finite pair current across the SIN interface, using a superconducting proximity model proposed by Geshkenbein and Sokol,[8] based on the time-dependent Ginzburg-Landau theory for gapless superconductors.

An alternative model to explain the large conductance enhancement in terms of phase coherent electronic transport was given by van Wees *et al.*,[9] and Beenakker,[10] Marmorkos *et al.*,[11] and Beenakker *et al.*[12] A disordered normal region, with elastic mean free path ℓ, is brought into contact with a superconductor, with a barrier present at the interface. The transparency of the barrier is taken to be much smaller than unity. In these models it is explicitly assumed that the pair potential in the normal metal $\Delta_N = 0$. Because the normal region is assumed to be shorter than the phase breaking length ℓ_φ, coherent backscattering of electrons and holes causes multiple coherent Andreev reflections. A crucial aspect in these models is the phase conjugation at $E = E_F$ and $B = 0$ in the Andreev reflection process, which is shown to result in an increase of the conductance at low bias. The magnitude of this effect can be calculated to be of order unity,[9–12] much larger than corrections due to weak localization, which are of the order $k_F\ell$. In the paper by Marmorkos *et al.*[11] the limit where the barrier has a transparency Γ close to 1 is also considered. In this case the opposite effect occurs; the conductance at low bias is reduced due to enhanced weak localization. This effect is again of the order $k_F\ell$. Numerical studies on mesoscopic, superconductor–normal-metal structures have also been performed by Takane and Ebisawa.[13,14] A similar model, using the quasiclassical Green's functions for nonequilibrium superconductors, is given by Zaitsev[15] and Volkov *et al.*[16,17]

In this paper, we present a systematic experimental study of Nb-p^{++}Si–normal-metal junctions. We varied both the junction length L and the material of the normal-metal counterelectrode, in order to understand the observed deviations from the classical BTK model.

II. EXPERIMENTAL SETUP AND GENERAL RESULTS

To study coherent backscattering in superconductor–normal-metal junctions, we need a system where the normal metal is both disordered, with elastic mean free path ℓ, and has a length L shorter than the phase breaking length ℓ_φ:

$$\ell < L < \ell_\varphi. \tag{1}$$

We used metallic p^{++}Si as the normal metal, and Nb as the superconductor. Our samples are based on Si membranes. They are fabricated using a selective, anisotropic etchant, which stops at the high boron concentration (8×10^{19} cm^{-3}) defined by ion implantation.[18] Different membrane thicknesses can be defined using different B-implantation profiles. At the Nb-Si interface a barrier is present. This barrier has two causes: a Schottky barrier, which has a very thin and nonuniform depletion layer due to the high doping level, and a barrier as a result of Fermi-velocity mismatch in the two materials. At the high doping levels used in this system, the standard Schottky barrier theory is no longer valid, because the calculated depletion length becomes comparable to the separation of the B acceptor ions, so the continuum model breaks down. The barrier strength obtained from experiment, $Z \simeq 2$, is very close to the theoretical minimum as calculated from Fermi-velocity mismatch, $Z_{\min} = \sqrt{(1-r)^2/4r} \simeq 1.3$, where r is the ratio of the Fermi velocities in the two materials. Following the analysis of van Huffelen *et al.*,[19] the elastic mean free path is estimated at $\ell \simeq 5$ nm, where we used for the bulk resistivity at 4.2 K a value of $\rho = (7.7 \pm 1.0) \times 10^{-4}\ \Omega$cm. For a schematic picture of the samples, and of the sample geometry, see Fig. 1. From previous experiments by van Huffelen *et al.*[20,19] we learned that the inelastic mean free path for electrons in the Si obeys $\ell_{\rm in} \gg L(= 50$ nm), as is clear from the high orders of multiple Andreev reflections. In a first approximation we can assume that the phase coherence length $\ell_\varphi \simeq \ell_{\rm in}$.

We used three different samples, whose properties are listed in Table I, together with some experimental results. The first type (sample A) are 500 nm thick Si membranes with Nb electrodes on both sides. Following the Kupriyanov-Lukichev theory,[21] we expect the supercurrent in these junctions to be negligibly small. Typical curves are given in Fig. 2. A sharp peak near $V = 0$ in the differential conductance is observed. This is not a precursor of a supercurrent, since it does not exhibit a Fraunhofer diffraction pattern in the magnetic-field dependence (not shown), and instead of developing into a true supercurrent, it saturates at temperatures below 100 mK (see the inset of Fig. 2). In some samples, a small feature can be seen at $V \simeq 0.28$ mV, as indicated by the arrows in Fig. 2. In most samples it is absent, and it is therefore believed to be an artifact, of unknown origin.

The conductance enhancement due to coherent backscattering is expected to be maximal for $\ell_\varphi \gg L$, and, because it is uncertain whether $\ell_\varphi > 500$ nm, we also studied thin (50 nm) membranes. For the superconducting top electrode we still used Nb, but we replaced the Nb of the bottom electrode by either Al (sample B), or W (sample C). Although Al becomes superconducting below $T_c = 1.18$ K, sample B did not show a supercurrent, presumably due to somewhat higher barriers at the Nb-Si and the Si-Al interfaces. These higher barriers are

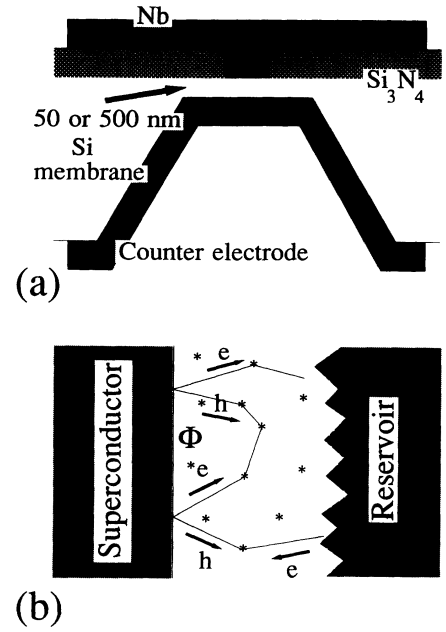

FIG. 1. Schematic picture of the junctions (a). A degenerately B-doped Si membrane ($N_{\rm B} = 8 \times 10^{19}$ cm^{-3}), with $L = 500$ nm and two superconducting Nb electrodes (sample A), or $L = 50$ nm and a normal-metal counterelectrode of Al (sample B) or W (sample C). (b) shows the geometry used in the model by van Wees *et al.*,[9] a superconductor in contact with a disordered normal conductor. For a detailed explanation, see the text.

TABLE I. Basic sample properties.

Sample	A	B	C
Counterelectrode	Nb	Al	W
$T_{c,E}$ (K)	9.2	1.18	0.015
L (nm)	500	50	50
Contact			
area (μm^2)	12	100	36
R_{c1} ($\Omega\,\mu$m^2)[a]	5	300	540
R_{c2} ($\Omega\,\mu$m^2)[a]	5	300	1620
low voltage conductance peak			
$\Delta G/G\|_{V=0}$ (%)	10	10	15
width (mV)	0.1	0.3	0.6
lowest conductance (Ω^{-1})[b]	0.34	9.85×10^{-3}	1.06×10^{-2}
$G_N/G\|_{V=0}$[c]	5	1.7	1.5

[a] $R_{c1,c2}$ is defined as the contact resistance multiplied by the contact area defined by lithography.

[b] The value of $dI/dV|_{V=0}$, without any conductance enhancement, is extrapolated from the tunnel curve [this is $(R_{\rm NS}^{\rm class})^{-1}$ from Ref. 12].

[c] The depth of the tunnel dip, where G_N is the normal state conductance at $V > \Delta/e$, and $G|_{V=0}$ is the lowest conductance as extrapolated from the tunnel curve.

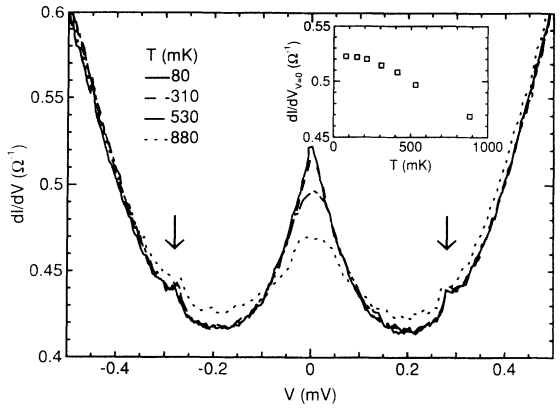

FIG. 2. Differential conductance as a function of voltage, for a thick membrane (500 nm), with two Nb electrodes, measured at 95 mK. The arrow points to a small conductance peak at nonzero voltage, which appears in some samples. In the inset the temperature dependence of the zero voltage bias conductance is plotted, showing a saturation at low temperatures.

due to the fabrication, and they are also present in sample C. Due to the presence of these barriers, the normal state resistance R_N, at voltage $V > \Delta/e$, is higher.

The differential conductance of sample B is shown in Fig. 3, for different temperatures (a) and for different applied magnetic fields (b). Despite the lower conductance as a result of the barriers, the conductance enhancement at low voltage bias is of the same order as for sample A. As can be seen from Fig. 3(a), there is a saturation in the height of the conductance peak. When the temperature is decreased from 170 mK to 70 mK, the peak height is not increased further. Analogous to the supercurrent in SNS junctions, the effect is expected to saturate when the coherence length $\xi(T) = \sqrt{\hbar D/kT}$ exceeds the junction length L. A further discusion will be given in Sec. III. In the inset of Fig. 3(a) the full curve up to voltages well above Δ_{Nb}/e is given, for the lowest temperature measured at. It shows standard SIN tunneling behavior, except for the small peak around $V = 0$. From Fig. 3(b) one can see that not only the zero voltage conductance peak is suppressed, but also the width of the tunnel dip is decreased with increasing magnetic field, due to the H dependence of the superconducting gap, of both the Nb and the Al. The abrupt change from 100 to 120 mT is a result of exceeding the critical field of the Al, which reduces the width of the tunnel dip from $\Delta_{Nb} + \Delta_{Al}$ to Δ_{Nb}. The tunnel dip appears broader than $\Delta_{Nb}/e = 1.5$ meV because approximately half of the voltage drop takes place at the Si-Al interface.

Figure 4 shows the differential conductance of sample C, Nb-Si-W, again for different temperatures (a) and applied magnetic fields (b). Although from Fig. 4(a) a saturation of the conductance enhancement is not clearly visible, it cannot be excluded from the presented data. Saturation could very well take place somewhere within the temperature range of 195–100 mK. Another important notion that can be extracted from this figure is that the temperature dependence of the enhanced conductance peak is not due to simple thermal smearing (convolution with the Fermi function). This would both lower and broaden the peak, whereas Fig. 4(a) only shows a decrease in height. This phenomenon, which can also be seen in Fig. 2, is not yet understood. The dependence on magnetic field, shown in Fig 4(b), has the same behavior as for the Al sample (B); both the zero voltage conductance peak height, and the tunnel dip width are reduced with increasing magnetic field. The magnetic field that is needed to destroy the conductance enhancement is somewhat larger than for sample B. This is also true for the temperature and the voltage up to which the conductance enhancement is present. For this sample the Nb-Si interface has a barrier comparable to that of sample B, whereas the Si-W barrier is somewhat higher than the Si-Al barrier. Therefore a larger portion of the voltage drop occurs at this second barrier, and both the tunnel dip and the conductance enhancement peak at low bias will appear broader. In all samples A–C the measured

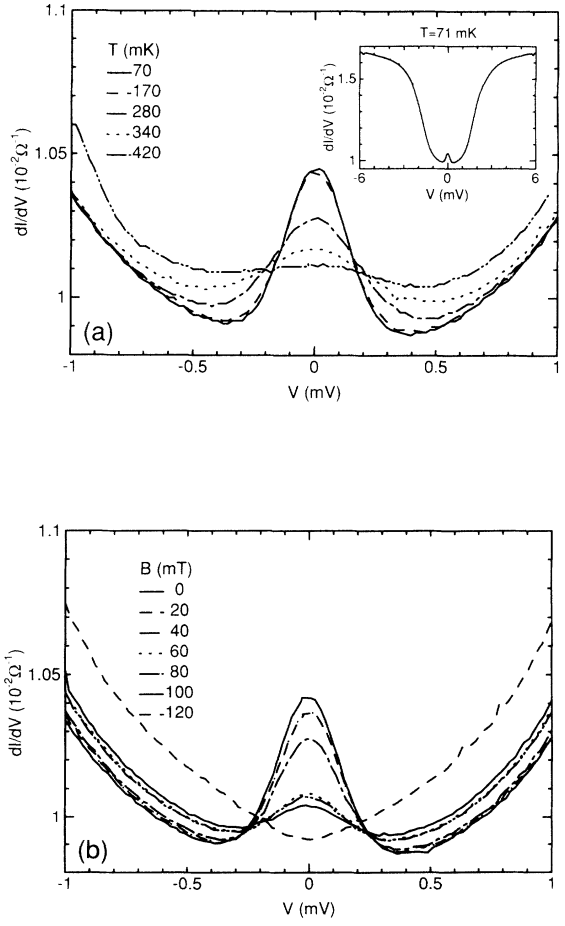

FIG. 3. Differential conductance as function of voltage, for a Nb-Si-Al junction, for various temperatures (a), and magnetic fields (b). The inset of (a) shows the overall conductance curve for the lowest temperature. In this inset the small peak at zero voltages can easily be identified as a small deviation from the normal tunnel curve. For this sample the contact hole in the Si_3N_4 layer is 10×10 μm^2.

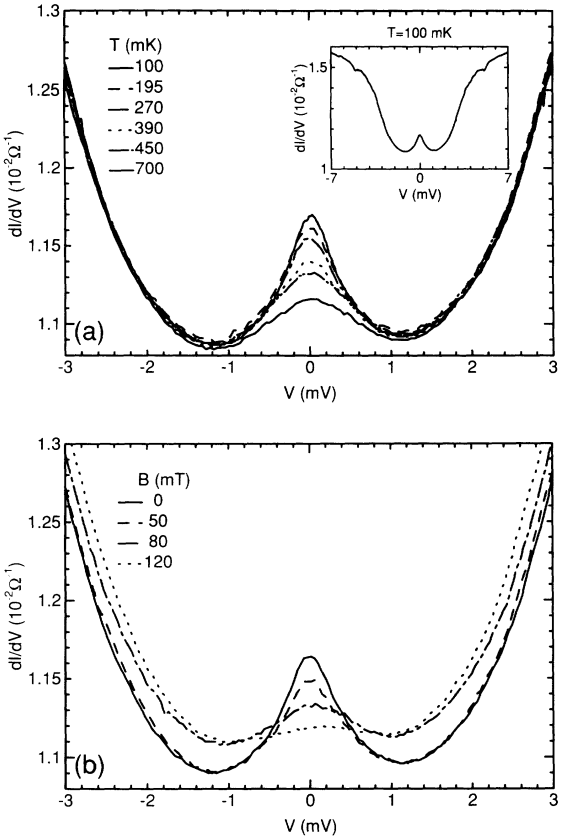

FIG. 4. Differential conductance as a function of voltage for a Nb-Si-W junction, for various temperatures (a), and magnetic fields (b). The inset of (a) shows the overall conductance curve for the lowest temperature. For this sample the contact hole in the Si_3N_4 layer is 6×6 μm^2.

correction of the zero voltage conductance $(\Delta G/G|_{V=0})$, with respect to the BTK model, is of the order 10–15 %, which is a very large correction as compared to the small corrections in weak localization.

III. COMPARISON TO THEORY

Van Wees *et al.*,[9] and Beenakker and co-workers[10–12] describe the electronic transport in a disordered SIN structure (disordered N) using a scattering matrix formalism. A superconductor is brought into contact with a disordered semiconductor ($\ell, \xi < L$), with a low transparent barrier at the interface. The coherence length ξ is the distance over which there is a correlation between electrons and holes in the semiconductor, as a result of Andreev reflections at the SIN interface. In general, this coherence length $\xi = \xi(T)$ is temperature dependent. There is no pair potential induced in the normal region ($\Delta_N = 0$), since it is assumed that electron-electron and electron-phonon interactions in the normal metal are negligible. A further assumption of both models is that there are no inelastic scattering or phase breaking processes ($L \ll \ell_\varphi$). Figure 1(b) shows the path of an incoming electron, which can be either normal or Andreev reflected at the SIN interface. If the electron is normal reflected, there is a good chance it will hit the SIN interface again after some path $\ell_{\rm path}$. The holes formed in both events can interfere, where their phase difference is given by[9]

$$\Delta\varphi = \frac{2E\ell_{\rm path}}{\hbar v_F} + 4\pi\frac{BA}{\phi_0}. \tag{2}$$

A is the area enclosed by the path $\ell_{\rm path}$ and B is the applied magnetic field. At $E = E_F$ and $B = 0$ the interference will be constructive and independent of path, and therefore result in an enhancement of the Andreev reflection probability. Coherent effects will be reduced if the average phase difference $\langle\Delta\varphi\rangle$ is of the order of 2π. Using $\langle\ell_{\rm path}\rangle \approx 0.35\ell/T_n$ as the average path length, where $T_n \approx \ell/L$ is the transmission probability of the middle region, and $\sqrt{\langle A^2\rangle} \approx 12\ell^2$ as the rms average area, we can therefore define[9] the critical voltage $eV_c = \frac{1}{2}\hbar v_F/\ell$ for which the enhanced conductance is suppressed. In an actual sample the single loop schematically shown in Fig. 1(b) can be extended to several loops, and, in the particular case that $T_n = 0.1$, the critical voltage V_c is modified to $V_c^{\rm eff} \approx 0.05V_c$. Substituting the specific parameters of our samples, $eV_c^{\rm eff} \approx 2.9$ meV, and for the critical magnetic field $B_c = 0.042\phi_0/\ell^2 = 6.9$ T. Obviously those numbers are much larger than the observed values. We therefore conclude that the average path length $\ell_{\rm path}$ and enclosed area A are larger by an order of magnitude. Marmorkos *et al.*,[11] who apply a more adequate description of impurity scattering than van Wees *et al.*, also give expressions for the critical voltage and magnetic field. Again inserting the parameters of the Si we get $eV_c = \frac{\pi}{2}\hbar v_F\ell/L^2 = 0.29$ meV and $B_c = \phi_0/LW = 20$ mT, where we used a junction length L of 50 nm, and a contact width W of 4 μm. The expression for the critical field B_c, however, is only valid for $W < L$. Furthermore, we also need to take into account the penetration of the magnetic field into the superconductor. Inserting $L = 50$ nm $+ \lambda_{\rm London} = 100$ nm and $W = 400$ nm, we find $B_c = 100$ mT. This value for W is still large compared to the length L, but the very good agreement with experiment suggests that this value is quite reasonable. If we try to compare this model to sample A, Nb–Si (500 nm)–Nb, we find much smaller values for V_c and B_c than from the experiment. This implies that the effective length $L^{\rm eff}$ for coherent effects is not the junction length $L = 500$ nm, but shorter. Comparing the height of the effect, Marmorkos *et al.* get a correction on the conductance $G_{\rm NS}|_{V=0}$ of the order unity. The experiments show a correction of 10–15 %, which is slightly smaller.

Very recently Beenakker *et al.*[12] presented calculations on the (zero voltage bias) resistance for different lengths L of the normal metal. The key result of their paper, for the transmission probability $\Gamma \ll 1$, is given by

$$\langle R_{\rm NS}\rangle = \frac{h}{2e^2N}\frac{\ell}{L}\Gamma^{-2} \quad \text{if } \Gamma L/\ell \ll 1, \tag{3a}$$

$$\langle R_{\rm NS}\rangle = \frac{h}{2e^2N}\left(\frac{L}{\ell} + \Gamma^{-1}\right) \quad \text{if } \Gamma L/\ell \gg 1, \tag{3b}$$

to be contrasted with the classical resistance (not taking into account phase coherent Andreev reflection)

$$R_{\rm NS}^{\rm class} = \frac{h}{2e^2 N}\left(\frac{L}{\ell} + 2\Gamma^{-2}\right) \tag{3c}$$

where $N = A/(\frac{1}{2}\lambda_F)^2$ is the number of available modes. As a result of phase coherence of electrons and holes across the entire sample, the classical resistance $R_{\rm NS}^{\rm class}$ is, for $\Gamma L/\ell \gg 1$, modified to $\langle R_{\rm NS}\rangle$ as given in Eq. (3b). As an example we will apply this model to sample A, Nb–p^{++}Si (500 nm)–Nb. The advantage of sample A is that is has two almost identical interfaces, so the $R_{\rm NS}$ of a single interface is simply the total resistance (at zero bias) divided by 2. From Fig. 2 we get (for the lowest temperature) $\langle R_{\rm NS}\rangle = 0.96\ \Omega$, and an interpolation of the tunnel curve gives $R_{\rm NS}^{\rm class} = 1.47\ \Omega$. Using $L/\ell = 100$, we get from the ratio $\langle R_{\rm NS}\rangle/R_{\rm NS}^{\rm class} = 0.653$ a value for $\Gamma = 0.18$. With Eqs. (3c) and (3b) we calculate, using $\Gamma = 0.18$ and N=(contact area)$/(\frac{1}{2}\lambda_F)^2$, $R_{\rm NS}^{\rm class} = 0.97\ \Omega$ and $\langle R_{\rm NS}\rangle = 0.63\ \Omega$. The contact area in these samples is defined as 12 μm^2 (see also Table I). These values are very close to the experimental values, the small discrepancy being mainly due to the uncertainty of the effective contact area. According to this model the effect would be much stronger in the 50 nm samples, B and C, since the ratio $\langle R_{\rm NS}\rangle/R_{\rm NS}^{\rm class}$ is reduced significantly when L/ℓ is changed from 100 to 10, and $\Gamma = 0.18$ kept constant. In Fig. 3 and Fig. 4 the effect is shown to be of the same order as in sample A. A nonuniform interface, leading to a smaller effective contact area, could account for a reduction of the conductance enhancement. This is also in agreement with the larger contact resistance in samples B and C, (see Table I).

Calculations, using quasiclassical Green's functions for nonequilibrium superconductors, are given by Volkov and co-workers.[16,17] Although the theoretical approaches are quite different, they yield qualitatively similar results. In some cases it has been verified that the two approaches also agree in detail (Marmorkos *et al.*[11]) Volkov *et al.* model a double-barrier SININ′ structure, for which the current can be expressed as

$$I = \frac{1}{eR_N}\int_0^\infty \mathcal{D}(E)\mathcal{F}(E)\partial E, \tag{4a}$$

$$\mathcal{D}(E) = \frac{r_1 + r_2 + 1}{\frac{r_1}{M_1(E)} + \frac{r_2}{M_2(E)} + \frac{1}{L}\int_0^L \frac{\partial x}{M_t(E,x)}}, \tag{4b}$$

$$\mathcal{F}(E) = \frac{1}{2}\left[\tanh\left(\frac{E+eV}{kT}\right) - \tanh\left(\frac{E-eV}{kT}\right)\right]. \tag{4c}$$

$\mathcal{D}(E)$ given in Eq. (4b) is the energy-dependent transmission probability of the entire junction. In general, the analytical expressions for $\mathcal{D}(E)$ are very complicated; however, in certain limits, it is possible to calculate $\mathcal{D}(E)$ numerically. In Eq. (4) $r_{1,2}$ is defined as the barrier resistance $R_{1,2}$ over the bulk resistance R, where the normal state resistance $R_N \equiv R_1 + R_2 + R$. $M_1 = [\nu\nu_s + \eta\eta_s](x_1)$ is a function of E, at the SIN boundary ($x = x_1$), which combines the normalized density of states in the superconductor S and the normal metal N. $M_2 = \nu(x_2)$ is determined from the density of states ν at the NIN′ boundary ($x = x_2$), where it is assumed that the density of states in N′ is constant. $M_t(x) = \nu(x)^2 + \eta(x)^2$ is dependent on the two position-dependent densities of states in N, ν and η. ν_s and η_s are taken for BCS superconductors, whereas ν and η have to be determined numerically (for details, see Ref. 17). Calculations for the low transparency limit ($r_1, r_2 \gg 1$), where the resistance of the middle layer can be neglected, are shown in Fig. 5. This limit is only valid for samples B and C, not for sample A. As can be seen, there is a very good resemblance to the differential conductance curves obtained from the experiment.

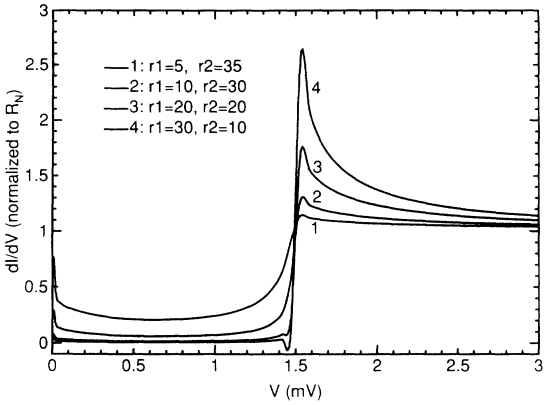

FIG. 5. Calculated normalized differential conductance as a function of applied voltage, according to the model by Volkov *et al.* (Ref. 17). $r_{1,2} = R_{1,2}/R$, where $R_{1,2}$ is the interface resistance and R the resistance of the bulk. For the curves shown, $\Delta = 1.5$ meV and $T = 100$ mK.

From previous measurements[20,19] it was already recognized that the Nb-Si contact in our devices is highly nonuniform. Van Huffelen *et al.* had to assume an effective area of only 2–3 % of the defined area, in order to get agreement between the calculated and measured normal state resistances. The ratios $r_{1,2}$ are defined as the contact resistance $R_{1,2}$ over the resistance R of the middle region. For a uniform interface, the barrier resistance is directly proportional to its transparency, leading to a unique value for $r_{1,2}$, but, since our barriers are nonuniform, it is not straightforward what values to choose for the ratios r_1 and r_2. This hinders an exact fit of the experiment, since in the model a uniform barrier is assumed at both interfaces.

IV. CONCLUSIONS

We have observed experimentally an enhancement of the conductance of Nb-p^{++}Si contacts, at low voltage bias ($eV \ll \Delta_{\rm Nb}$) and temperatures well below the superconducting transition temperature T_c of Nb. Qualitatively we can explain our results by assuming multiple Andreev reflections due to coherent backscattering, as proposed by van Wees *et al.*[9] A more quantitative com-

parison can be made by using the model of Beenakker[10] and Marmorkos *et al.*,[11] who apply a more adequate description of impurity scattering. Using this model, together with the specific parameters of our samples, values for V_c and B_c, the critical voltage and magnetic field above which the effect is diminished, are found to be in good agreement with the experiment. Regarding the amplitude of the corrections, Beenakker *et al.*[12] calculate the zero voltage bias resistance as function of the transmission probability Γ of the SN interface, for different lengths L of the normal region. These calculations are in good comparison with sample A [Nb–Si (500 nm)–Nb], but predict larger corrections for sample B [Nb–Si (50 nm)–Al] and C [Nb–Si (50 nm)–W] than obtained from the experiment.

A different theoretical approach is used by Zaitsev[15] and Volkov *et al.*[16,17] for our specific system yielding similar results.

Discrepancies between theory and experiment cannot be resolved conclusively by the present experiment in view of the inhomogeneity of the interface. It is therefore essential to study the influence of the shape of the interface barriers on the electronic properties of these systems.

ACKNOWLEDGMENTS

The authors would like to thank M. J. de Boer for teaching them how to prepare the samples, and A. V. Zaitsev and A. F. Volkov for useful discussions. This work is part of the research program of the stichting voor Fundamenteel Onderzoek der Materie (FOM), which is financially supported by the Nederlandse organisatie voor Wetenschappelijk Onderzoek (NWO).

* Present address: Kamerlingh Onnes Laboratory, University of Leiden, Postbox 9506, 2300 RA Leiden, The Netherlands.

[1] A. F. Andreev, Zh. Eksp. Teor. Fiz. **46**, 1823 (1964) [Sov. Phys. JETP **19**, 1228 (1964)].
[2] G. E. Blonder, M. Tinkham, and T. M. Klapwijk, Phys. Rev. B **25**, 4515 (1982).
[3] M. Octavio, M. Tinkham, G. E. Blonder, and T. M. Klapwijk, Phys. Rev. B **27**, 6739 (1983).
[4] T. M. Klapwijk, G. E. Blonder, and M. Tinkham, Physica B&C **109&110B**, 1657 (1982).
[5] K. Flensberg, J. B. Hansen, and M. Octavio, Phys. Rev. B **38**, 8707 (1988).
[6] A. Kastalsky *et al.*, Phys. Rev. Lett. **67**, 3026 (1991).
[7] G. Bergmann, Phys. Rep. **107**, 1 (1984).
[8] V. B. Geshkenbein and A. V. Sokol, Zh. Eksp. Teor. Fiz. **94**, 259 (1988) [Sov. Phys. JETP **67**, 362 (1988)].
[9] B. J. van Wees, P. de Vries, P. Magnée, and T. M. Klapwijk, Phys. Rev. Lett. **69**, 510 (1992).
[10] C. W. J. Beenakker, Phys. Rev. B **46**, 12 841 (1992).
[11] I. K. Marmorkos, C. W. J. Beenakker, and R. A. Jalabert, Phys. Rev. B **48**, 2811 (1993).
[12] C. W. J. Beenakker, B. Rejaei, and J. A. Melsen (unpublished).
[13] Y. Takane and H. Ebisawa, J. Phys. Soc. Jpn. **61**, 2858 (1992).
[14] Y. Takane and H. Ebisawa, J. Phys. Soc. Jpn. **61**, 1685 (1992).
[15] A. V. Zaitsev, Pis'ma Zh. Eksp. Teor. Fiz. **51**, 35 (1990) [JETP Lett. **51**, 41 (1990)].
[16] A. F. Volkov and T. M. Klapwijk, Phys. Lett. A **168**, 217 (1992).
[17] A. F. Volkov, A. V. Zaitsev, and T. M. Klapwijk, Physica C **210**, 21 (1993).
[18] W. M. van Huffelen, M. J. de Boer, and T. M. Klapwijk, Appl. Phys. Lett. **58**, 2438 (1991).
[19] W. M. van Huffelen *et al.*, Phys. Rev. B **47**, 5170 (1993).
[20] W. M. van Huffelen, T. M. Klapwijk, and L. de Lange, Phys. Rev. B **45**, 535 (1992).
[21] M. Y. Kupriyanov and V. F. Lukichev, Zh. Eksp. Teor. Fiz. **94**, 139 (1988) [Sov. Phys. JETP **67**, 1163 (1988)].

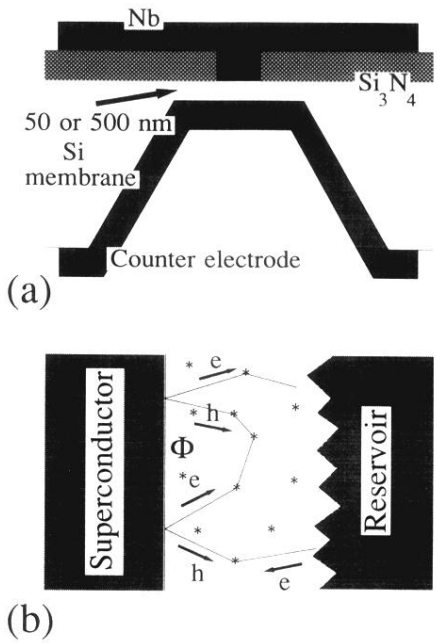

FIG. 1. Schematic picture of the junctions (a). A degenerately B-doped Si membrane ($N_B = 8 \times 10^{19}$ cm^{-3}), with $L = 500$ nm and two superconducting Nb electrodes (sample A), or $L = 50$ nm and a normal-metal counterelectrode of Al (sample B) or W (sample C). (b) shows the geometry used in the model by van Wees *et al.*,[9] a superconductor in contact with a disordered normal conductor. For a detailed explanation, see the text.